Research paper

Nuclei carrying entrapped air are the most likely starting points for eye formation

Dominik Guggisberg , Walter Bisig , Marie-Therese Fröhlich-Wyder *

Agroscope, Schwarzenburgstr. 161, CH-3003, Bern, Switzerland

ARTICLE INFO

ABSTRACT

Eye nuclei with structural elements, such as hay particles with capillary structures, have been hypothesised to be a prerequisite for eye formation in cheese. Such eye nuclei act as microscopic air bubbles in capillaries that are trapped in the cheese matrix, into which the CO_2 diffuses to initialise the eye formation process. To verify this hypothesis, this experimental study evaluated the impact of synthetic hollow fibres and tube pieces with standardised capillary properties instead of hay particles. The results clearly showed that both synthetic hollow fibres and tube pieces with capillary cavities were highly effective in the process of eye formation and were found in cross-sectional microscopic images related to the cheese eyes. The control cheeses without any fibres or tube pieces tended to have a very low number of eyes and therefore showed cracks because the formed CO_2 was not able to diffuse into non-existent eye nuclei.

1. Introduction

The size, number, shape, and distribution of eyes (cheese openings) in Swiss-type cheeses and other cheese varieties are meaningful quality parameters. Eye formation depends primarily on the timing, amount, and intensity of CO_2 formation, its diffusion properties within and out of the cheese, the presence of eye nuclei, and the texture and temperature of the cheese. Eye nuclei act as microscopic air bubbles in capillaries that are trapped in the cheese matrix, into which the CO_2 diffuses to enable the eye formation process in cheese. The capillary effect is a phenomenon in which liquids rise or fall in narrow tubes or porous materials due to the interplay of adhesive and cohesive forces and surface tension. When a capillary is moistened with water or milk from both sides at the same time, an enclosed air bubble is formed.

In Swiss-type cheese, eye formation is primarily the result of CO_2 production by propionic acid bacteria (PAB) during warm room ripening (approximately 60 days at 20–24 °C for Emmentaler PDO). However, smaller amounts of CO_2 are produced earlier during lactic acid fermentation and citrate degradation at the beginning of the ripening process. Flückiger (1980) indicated that eye formation in Emmentaler PDO begins at about half the CO_2 saturation of approximately 36 mmol kg^{-1}. Martley and Crow (1996) found that saturation of the cheese matrix with CO_2 (>18–36 mmol kg^{-1}) is a prerequisite for eye formation. Eye formation can occur only with a sufficient CO_2 formation rate and

relatively low CO_2 diffusion out of the cheese. CO_2 diffusion out of the cheese can be tracked by gas volume monitoring, as illustrated by Bisig et al. (2019) and Wenzel et al. (2018), and the dynamics of CO_2 production and losses can be estimated. Once sufficient eyes have developed during warm room ripening (~60 days), CO_2 production is reduced automatically when the temperature is lowered to 10–13 °C.

The CO_2 formation in cheese is affected by the added starter and adjunct cultures, the indigenous microbiota, salt concentration, ripening temperature, and ripening time (Acerbi, Guillard, Aliani, et al., 2016; Fröhlich-Wyder et al., 2025). Due to the inhibitory effect of salt on the PAB culture in that study (Acerbi, Guillard, Guillaume, et al., 2016), the CO_2 formation rate decreased linearly with increasing salt content while it increased with temperature. Bisig et al. (2019) analysed the effects of NaCl on eye formation and PAB growth in cheese. PAB was inhibited by increased NaCl, and the experiment showed that the strain-specific salt sensitivity of PAB strongly influenced eye formation in Swiss-type cheese. The eyeless border zone was mainly influenced by CO_2 diffusion out of the cheese, propionic acid fermentation, and cheese firmness.

Testing the progression of eye formation is traditionally carried out by listening to the type of sound resonating while tapping on the cheese's surface with a special hammer, by visual inspection of a small cylinder of cheese using a cheese trier, or by viewing a section of a cheese cut into halves. However, newer methods involving non-invasive image acquisition using X-ray computed tomography (CT) (Abrahamsen et al., 2006;

Table 1

Experimental design for model Emmentaler cheese produced with skimmed and microfiltered raw milk[a]. Cheeses 1–8 and 9–16 were produced on day 1 and day 2, respectively.

Cheese	Variant	PP[b] hollow fibres or PEEK[c] tube pieces Type, amount per 90 L of milk, inner diameter, length
1	Control	—
2	PEEK1 (low)	*HPLC tubes, 1.1 g (low), Ø: 0.13 mm, length: 2–3 mm*
3	PEEK2 (high)	*HPLC tubes, 2.3 g (high), Ø: 0.13 mm, length: 2–3 mm*
4	PP hollow fibre, 6 mm	*Synthetic fibres, 0.17 g, Ø: ~10 μm, length:6 mm*
5	Control	—
6	PEEK1 (low)	*HPLC tubes, 1.1 g (low), Ø: 0.13 mm, length: 2–3 mm*
7	PEEK2 (high)	*HPLC tubes, 2.3 g (high), Ø: 0.13 mm, length: 2–3 mm*
8	PP hollow fibre, 6 mm	*Synthetic fibres, 0.17 g, Ø: ~10 μm, length:6 mm*

Cheese	Variant	PP fibres or PEEK tube pieces
9	Control	—
10	PEEK1 (low)	*HPLC tubes, 0.5 g (low), Ø: 0.18 mm, length: 2–3 mm*
11	PEEK2 (high)	*HPLC tubes, 1.4 g (high), Ø: 0.18 mm, length: 2–3 mm*
12	PP hollow fibre, 2 mm	*Synthetic fibres, 0.19 g, Ø: ~10 μm, length:2 mm*
13	Control	—
14	PEEK1 (low)	*HPLC tubes, 0.5 g (low), Ø: 0.18 mm, length: 2–3 mm*
15	PEEK2 (high)	*HPLC tubes, 1.4 g (high), Ø: 0.18 mm, length: 2–3 mm*
16	PP hollow fibre, 2 mm	*Synthetic fibres 0.12 g, Ø: ~10 μm, length:2 mm*

[a] Commercial UHT cream from two different manufacturers (Emmi or Cremo) was used for standardisation.
[b] Polypropylene.
[c] Polyetheretherketone.

Guggisberg et al., 2015; Schuetz et al., 2013; Schuetz, Guggisberg, Fröhlich-Wyder, & Wechsler, 2016) have been applied to quantitatively investigate eye formation in cheese, especially with regard to growth kinetics, size, number, spatial distribution, sphericity, ripening stages, and defects. The growth of an individual cheese eye was compared in an experiment using models and simulations (Laridon et al., 2020) based on Fick's law for mass transport (CO_2 diffusion in cheese) and Henry's law (solubility of CO_2 in cheese) for exchange at the eye–cheese interface. The model was consistent with the experiment in the core of the cheese and emphasised the significant influence of the CO_2 production rate and the amount of cheese material around the cheese eye.

Another aspect, the fat content of cheese, was recently studied by

Fröhlich-Wyder et al. (2023) in relation to the relative eye volume of Swiss-type cheese. Since CO_2 is soluble in both the aqueous and fat phases of cheese (Henry's law), it was found that increases in fat content have a significant ($p < 0.05$) inhibiting effect on the relative eye volume in semi-hard and hard cheeses. However, the CO_2 solubility capacity of each phase depends on the temperature (Jakobsen, Jensen, & Risbo, 2009). The solubility of CO_2 in renneted casein matrices was also studied by Lamichhane et al. (2021), who found it to be dependent on pH value, salt, temperature, partial pressure, and moisture-to-protein ratio. The CO_2 solubility of cheese samples decreased linearly with increasing temperatures and increased salt content in the moisture, while CO_2 solubility increased with rising pH values and partial pressure. A nonlinear relationship between CO_2 solubility and the moisture-to-protein ratio was observed.

Multiscale studies of eyes in Swiss-type cheeses were conducted by Huc, Moulin, Mariette, & Michon (2013) and Huc et al. (2014a, 2014b) to determine the relationship between the growth of eyes and the microstructure of the cheese mass around the eyes. Magnetic resonance imaging was combined with three microscopic techniques (light microscopy, confocal laser scanning microscopy, and scanning electron microscopy; macroscale to microscale) to determine the organisation of the fat and protein network in the cheese matrix around the cheese eyes. The curd granules appeared to be highly stretched around the openings.

The quantity and distribution of cheese eyes also depend highly on technological treatments, such as filtration, centrifugation, bactofugation, or microfiltration of cheese milk, as well as on cheese composition. Centrifugation and heat treatment of the cheese milk or the application of vacuum during moulding or pressing of the cheese induce lower numbers of eyes. In cheese varieties made from microfiltered milk, the number of eyes is generally much lower (Fragnière & Schafroth, 2004).

More than a century ago, Clark (1917) postulated that eye formation in cheese would occur at "preferred locations" and that it is similar to the phenomenon of crystallisation from a supersaturated solution, in which the onset of crystal growth is necessarily triggered by small "seeds" or "irregularities", and the size of the final crystals depends on the number of seeds added.

According to current knowledge, trace amounts of finely ground hay powder, when added to microfiltered milk, act as "eye-nuclei" and lead to the formation of eyes during cheese maturation in a dose-dependent

Table 2

Chemical composition of experimental Emmental cheeses at the end of the ripening period (100 days). After the Tukey-HSD test, the pH and NPN (data not shown) were no longer significant.

Cheese	Variant	Moisture [g 100 g⁻¹]	Total Nitrogen [g kg⁻¹]	Total volatile carbonic acids [mmol kg⁻¹]	pH [−]	Total lactate [mmol kg⁻¹]	Citrate [mmol kg⁻¹]
1	Control	35.5	47.5	100.7	5.58	103.8	n.d.
2	PEEK1 (low)	33.7	48.0	106.3	5.66	78.5	n.d.
3	PEEK2 (high)	35.6	46.9	118.8	5.65	98.9	n.d.
4	PP hollow fibre, 6 mm	34.0	48.3	124.1	5.65	112.3	n.d.
5	Control	33.6	48.1	174.0	5.70	20.7	7.2
6	PEEK1 (low)	33.2	48.6	122.0	5.64	76.3	n.d.
7	PEEK2 (high)	33.8	48.1	140.7	5.68	11.7	7.3
8	PP hollow fibre, 6 mm	35.1	47.7	97.8	5.57	97.2	n.d.
9	Control	35.7	47.4	100.1	5.56	123.4	n.d.
10	PEEK1 (low)	34.2	48.2	148.1	5.70	9.3	7.3
11	PEEK2 (high)	35.4	46.1	100.6	5.72	83.5	n.d.
12	PP hollow fibre, 2 mm	34.0	47.4	95.2	5.62	100.6	n.d.
13	Control	34.2	47.3	93.3	5.62	100.7	n.d.
14	PEEK1 (low)	33.3	47.3	110.5	5.68	82.9	n.d.
15	PEEK2 (high)	34.0	48.2	148.5	5.71	7.6	7.3
16	PP hollow fibre, 2 mm	36.1	47.0	101.6	5.58	106.3	n.d.
Two-way ANOVA[a]							
Fibre		n.s.	n.s.	n.s.	*	n.s.	n.s.
Production day		n.s.	n.s.	n.s.	n.s.	n.s.	n.s.

n.d.: not determined (detection limit in cheese: 0.25 mmol kg⁻¹), n.s.: not significant, *: $p < 0.05$, >0.01, **: $p < 0.01$, >0.001.
[a] Two-way ANOVA with factors fibre/tube pieces and production day. The ANOVA was calculated without interaction, as no interaction was significant.
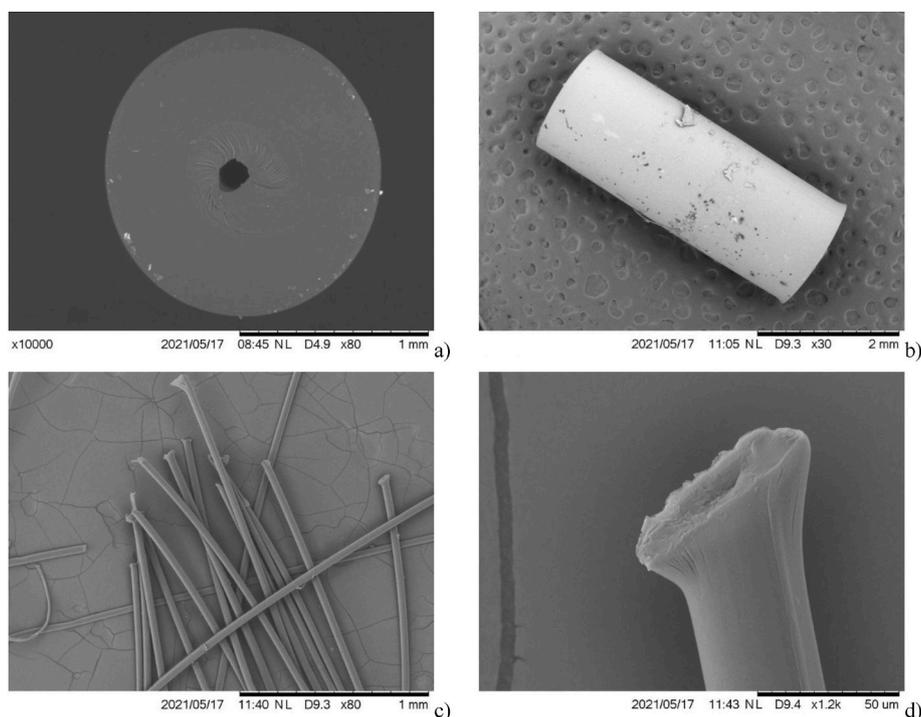
Fig. 1. Representations of PEEK HPLC tubings (a, b) and synthetic hollow fibres PP 450 DEN 50F, (c, d), analysed by SEM microscopy.

Table 3
Relative eye volume (in % of the cheese volume), and number of eyes per cheese.

Cheese	Variant	Relative eye volume [%]	Number of eyes per cheese [−]
1	Control	0.2	23
2	PEEK1 (low)	2.8	37
3	PEEK2 (high)	2.7	63
4	PP hollow fibre, 6 mm	2.9	160
5	Control	0.3	12
6	PEEK1 (low)	3.9	59
7	PEEK2 (high)	5.7	119
8	PP hollow fibre, 6 mm	0.6	13
9	Control	0.7	573[b]
10	PEEK1 (low)	2.4	43
11	PEEK2 (high)	2.5	94
12	PP hollow fibre, 2 mm	4.8	246
13	Control	0.3	28
14	PEEK1 (low)	2.3	44
15	PEEK2 (high)	5.7	125
16	PP hollow fibre, 2 mm	7.6	466
ANOVA[a]			
Fibre		**	**
Production day		n.s.	n.s.

n.s.: not significant, *: $p < 0.05, >0.01$, **: $p < 0.01, >0.001$.
[a] Two-way ANOVA with factors fibre/tube pieces and production day. The ANOVA was calculated without interaction, as no interaction was significant.
[b] High number due to mechanical opening defect during filling of the curd; not included in the statistical analysis.

manner (Guggisberg et al., 2015). Microscopic examination of microparticles of the hay powder showed that capillary structures were present in plant parts, such as leaves or stems, and that these microparticles were most likely effective structural elements that might act as eye nuclei and enable eye formation during cheese ripening. The probable

inclusion of tiny air bubbles in such capillaries decreases the necessary partial pressure to form an eye and allows the diffusion of CO_2 from the cheese mass into the microparticles. This was postulated as the probable explanation of these observations.

The aim of this study was, therefore, to investigate the experimental addition of microscopic and macroscopic synthetic fibres/capillaries to mimic hay powder particles in microfiltered cheese milk and thereby confirm the hypothesis of "eye nuclei" as a prerequisite of eye formation in Swiss-type cheese.

2. Materials and methods

2.1. Production of experimental Emmentaler cheese

Experimental Emmentaler cheese was prepared according to Guggisberg et al. (2015) by using skimmed and microfiltered (50 °C, 1.4 μm, 240 kPa) raw milk. Ultra-high temperature (UHT) treated cream (Emmi, Emmen, Switzerland or Cremo, Fribourg, Switzerland) was added to the microfiltered skim milk to reach a fat content of around 35 g kg^{-1}. Eight variants were produced in parallel from the same standardised milk (starting from 90 L of milk for each variant; the average cheese volume was around 6.5 L). Thus, cheeses 1–8 were produced on day 1 and cheeses 9–16 on day two. Instead of suspended hay particles, synthetic hollow fibres (Swicofil, Emmenbrücke, Switzerland) or pieces of high performance liquid chromatography (HPLC) tubes (Polyetheretherketone (PEEK), Agilent Technologies, Basel, Switzerland) were added experimentally to the curd during filling, submersed in whey, in the forms outlined in Table 1. Synthetic polypropylene hollow fibres (variant "PP fibre") were delivered in cut form (2 mm or 6 mm long, inner diameter: ~10 μm) by Swicofil (PP 450 DEN 50F, Emmenbrücke, Switzerland). The HPLC tubes (variant "PEEK" tube pieces) were cut into a length of 2–3 mm with a Thermo Scienctific Polymer Tubing Cutter (Fischer Scientific, Basel, Switzerland). The cut PEEK tube pieces and PP hollow fibres are presented in Fig. 1. A second run of eight experimental Emmentaler cheeses was produced the same week using the same procedure, as shown in Table 1, with slightly different amounts of synthetic fibres and tube pieces. After pressing (50 °C to > 25 °C, 1
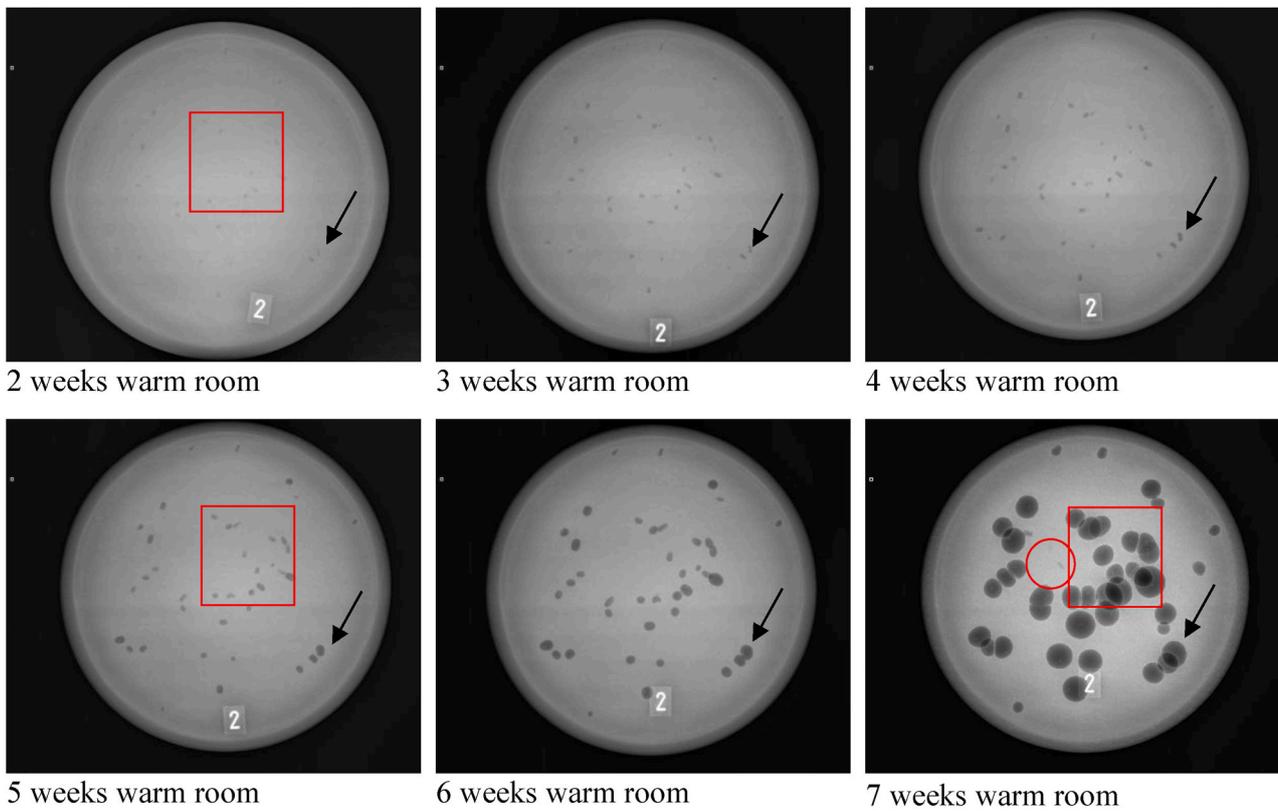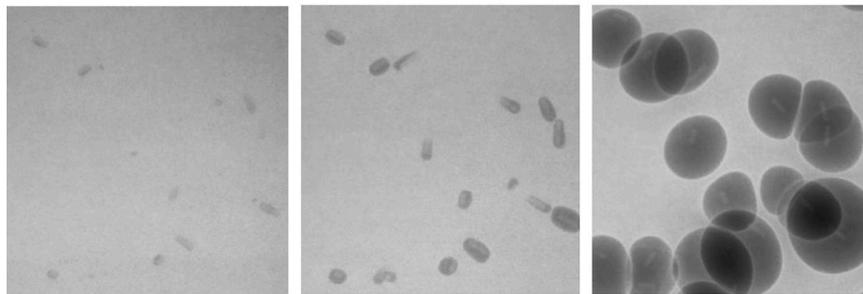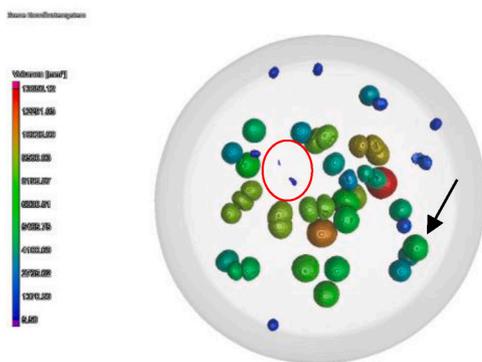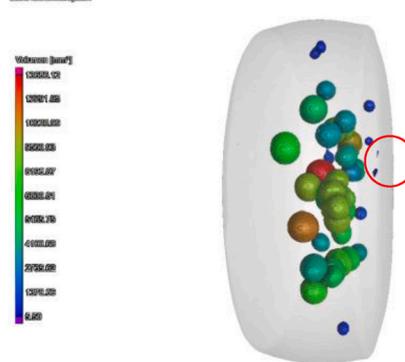
Fig. 2. 2-dimensional X-ray images of cheese 2 during warm room ripening (weeks 2–7) showing eye formation based on the added PEEK tube pieces. Eye formation started exactly at the sites of the added tube pieces, which had the effect of eye nuclei. The black arrows indicate three PEEK tube pieces, representing all others that have been added and around which the CO_2 formed cheese eyes starting from weeks 3–4. Enlarged sections of the images taken after 2, 5 and 7 weeks (red squares) show tube pieces and eyes, that had formed around the tube pieces (b). The red circle indicates a zone where no PEEK tubes were present, but cracks formed. The 3-dimensional image from the computed tomography (CT) images (c, d) showed that a crack was formed close to the surface. Additional to the lacking eye nuclei, the cheese texture is less viscoelastic, and therefore cheese eyes do not form properly. (For interpretation of the references to colour in this figure legend, the reader is referred to the Web version of this article.)

Anova, $F(3,11) = 7.47$, $p = 0.005$, $\eta_g^2 = 0.67$

Anova, $F(3,10) = 8.78$, $p = 0.004$, $\eta_g^2 = 0.72$
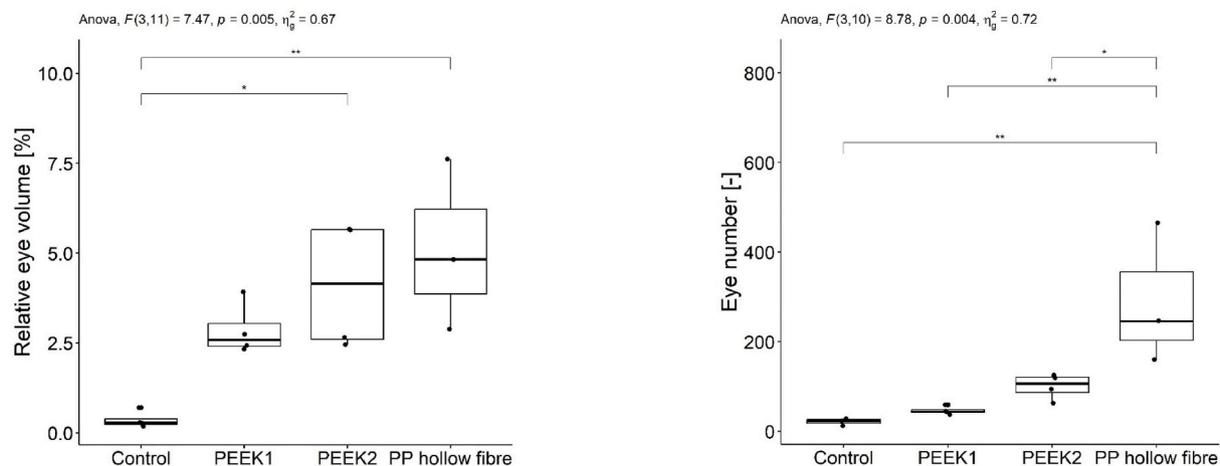
Fig. 3. Boxplots of relative eye volume and eye number as a function of the different synthetic hollow fibres or tube pieces. Cheeses 1–8 and cheeses 9–16 were produced on two different days, and two outliers (cheeses 8 and 9) were eliminated. The data were analysed using a one-way ANOVA, followed by Tukey post-hoc tests to perform multiple pairwise comparisons between groups (without effect of production day). Only significant differences are displayed in the figures; some data points are overlapping.

day), the cheeses were brine-salted (12 °C, 24 h) to achieve a salt content of around 5 g kg^{-1}. Ripening was carried out in the cold room (12 °C) for 10 days, then in the warm room for an additional 60 days at 22 °C (80 % relative humidity). After 70 days of ripening, the cheese samples were then stored at 12 °C prior to the analysis at the age of 100 days (mean reference values at 120 days for moisture: 353, and for fat: 310 g kg^{-1}, Guggisberg et al., 2015).

The 16 cheeses were specially labelled after production and during ripening to indicate that they were not approved for consumption. A risk analysis of the synthetic fibres for application in a pilot plant was carried out prior to the entire experiment.

2.2. Analysis of cheese pH after 4 h, 24 h, and at the end of ripening

Cheeses 1–16 were analysed for pH after 4 h and 24 h and at the end of the ripening period using a Metrohm instrument (Metrohm, Herisau, Switzerland). The instrument was calibrated once a day with standards at pH = 4 and pH = 7 (Merck, Darmstadt, Germany). All samples were analysed in duplicate (n = 2). The young cheese was analysed directly by penetrating the pH probe 5 cm into the cheese. For the ripened cheese, 2–5 g were grinded and filled compactly in a tube, where pH was measured.

2.3. Chemical analysis of cheese variants at the end of the ripening period

Moisture content was determined with the dry matter method (ISO 5534:2004/IDF 4:2004) by calculating the weight difference of the cheese sample after drying at 102 °C for 4 h. Total nitrogen (TN) and non-protein nitrogen (NPN) were analysed following ISO 8968-3: 2004/IDF 20-3: 2004 and ISO 8968-4: 2016/IDF 20-4: 2016, respectively. Soluble nitrogen at pH = 4.6 (SNpH4.6) was analysed using the Kjeldahl method, according to Collomb et al. (1990).

Volatile carboxylic acids (C1–C6) were analysed using gas chromatography and a flame ionisation detector with headspace technology after esterification with ethanol, as described by Badertscher et al. (2023). Total lactate was determined by ISO 8069/IDF 069 (2005). Citrate was analysed using the IDF Standard method (34C: 1992): *Cheese & processed Cheese products, Determination of Citric acid content (Enzymatic Method)*.

2.4. Analysis of cheese eyes by CT or X-ray

CT analysis was carried out at the end of the ripening after 3 months

following the experimental details according to Guggisberg et al. (2015) and Bisig et al. (2019). For the analysis of the raw CT data (DICOM format), VGSTUDIO MAX 2024.1 (Volume Graphics GmbH, Heidelberg, Germany) was applied. The relative eye volume indicates the total eye volume as a percentage of the total cheese volume.

X-rays were conducted using a CPI system (CPI, Ontario, Canada) with an X-ray tube XSTAR-74 from Comet (Comet, Niederwangen, Switzerland).

2.5. Visualisation of HPLC tubes and synthetic fibres

Synthetic fibres (PP fibres) and HPLC tubes (PEEK tube pieces) were visualised using a scanning electron microscope (SEM, Hitachi, Quantum Design GmbH, Pfungstadt, Germany). In cross-sectional views of cheese, PP fibres and PEEK tube pieces were visualised using a Keyence VHX-7000 digital microscope (Keyence, Mechelen, Belgium) or digital camera.

2.6. Statistical analysis

The experimental multifactorial design as shown in Table 1 provided replicates with a minimum number of 4 per categorial variable. We studied the effects of the factor hollow fibre/tube pieces (4 levels with "PEEK1" (N = 4), "PEEK2" (N = 4), "PP fibre" (N = 4) and "Control" (N = 4)) and of the factor production day (two levels "Day 1" and "Day 2", each N = 8). The effects of the two factors on the chemical composition of the cheeses were analysed using two-way ANOVA followed by Tukey-HSD post-hoc test using R (www.r-project.org, version: 4.5.0). Differences between the various factor levels were considered statistically significant at p ≤ 0.05. The experimental data for the relative eye volume and the eye number were analysed using either one-way (Fig. 3) or two-way ANOVA (Table 3) followed by Tukey-HSD post-hoc test. One-way ANOVA was chosen to show the impact of the main factor (hollow fibres and tube pieces) on eye formation in a clear way, since the production day had no effect.

3. Results and discussion

3.1. Chemical composition of the experimental Emmentaler cheese

The average fat content of all 16 cheese milk samples was 3.35 ± 0.06 % (w/w) and average fat/protein ratio was 1.03 ± 0.02 [-]. Cheeses 1–8 were produced on the first day, with the average pH value reaching
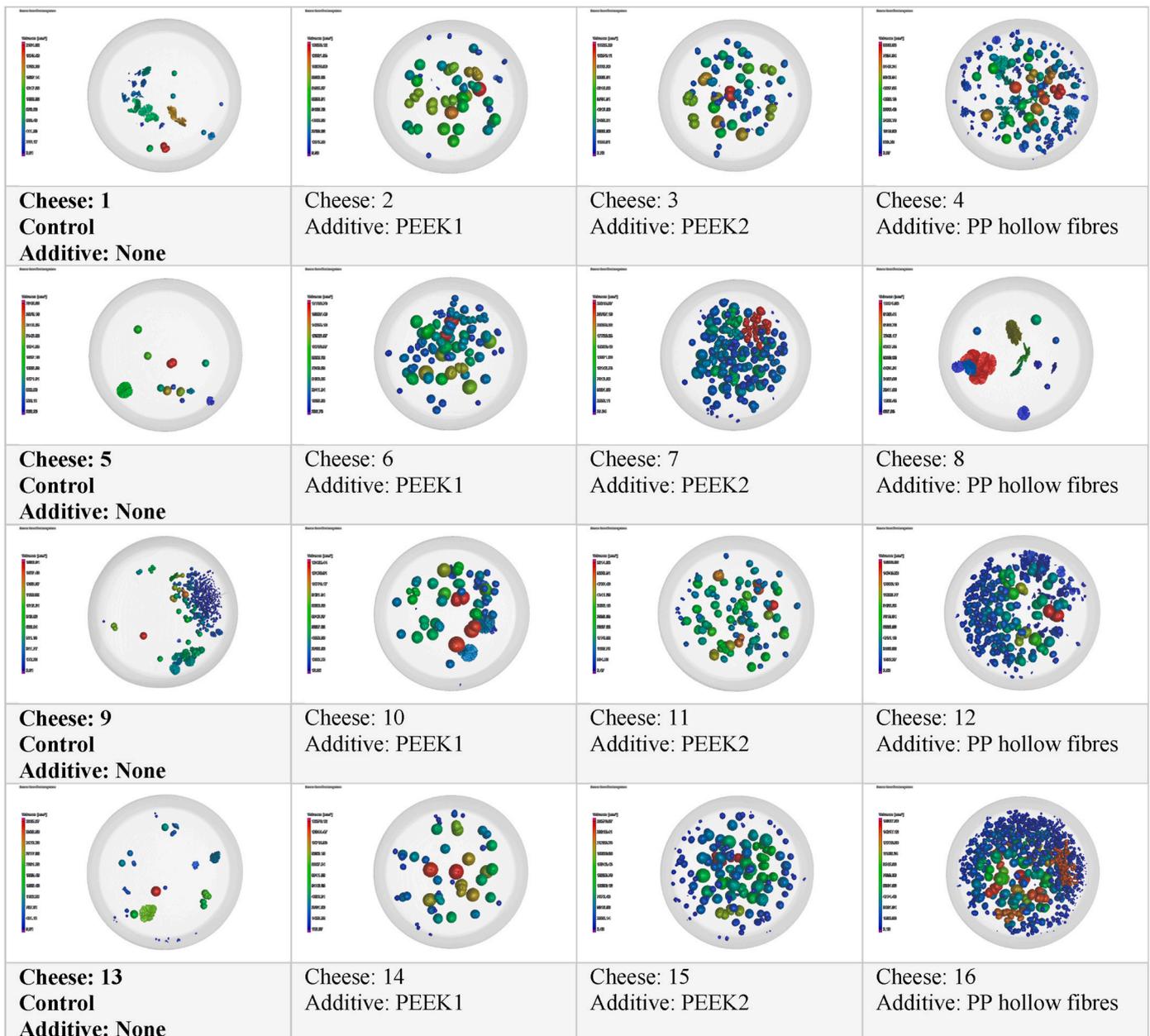
Fig. 4a. Cheese eyes visualised in the CT analysis (3D figures).

pH = 5.56 after 4 h and pH = 5.20 after 24 h. Cheeses 9–16 were produced on day two in the same week, and the average pH values after 4 h and 24 h were 5.52 and 5.18, respectively. No significant difference was found in terms of pH value (after 24 h) or fat and protein content of the cheese milk. This suggests that all 16 Swiss-type cheeses underwent similar lactic acid fermentation (Table 2).

Additional chemical composition parameters of the experimental Emmentaler cheeses at the end of the ripening period are presented in Table 2. We also analysed TN, NPN, and SNpH4.6 which were in the expected range: TN = 47.6 g kg^{-1}, NPN = 5.94 g kg^{-1}, and SNpH4.6 = 11.56 g kg^{-1}. Even though the moisture content (332–361 g kg^{-1}) varied slightly, no significant influence of the experimental parameters on proteolysis was found. A two-way ANOVA analysis revealed that with two exceptions (pH and NPN), the chemical differences between the factor fibre/tube pieces were not significant. Low significance was found for pH and NPN, which disappeared following a Tukey-HSD test; therefore, pH and NPN were considered irrelevant for further evaluation in this study.

We further found that citrate was completely metabolised in most cheeses. Usually, facultative heterofermentative lactobacilli (FHL) originating from the raw milk or added as a secondary culture are responsible for complete citrate metabolism (Fröhlich-Wyder et al., 2002). This is confirmed by the higher contents of formic acid in the respective cheeses (all variants except 5, 7, 10, and 15; data not shown). However, neither the addition of an FHL culture nor the use of raw milk was applied in the present study. We then considered contamination of the vat milk with FHL from the cheese dairy environment. Only in the four variants 5, 7, 10, and 15 did citrate remain nearly untouched, with the consequence of stronger lactate fermentation by PAB leading to higher contents of acetic and propionic acid (Table 2, column total volatile carboxylic acids). It is known that FHL are used to control and slow down propionic acid fermentation in some Emmentaler type cheeses (Fröhlich-Wyder et al., 2002). Section 3.3 presents our analysis of the influence of FHL on the eye volume of the respective cheeses, since CO$_2$ is simultaneously produced during propionic acid fermentation.

Fig. 4b. Cross sectional views of cheeses.

3.2. Monitoring eye formation using a 2-dimensional X-ray during the ripening period of up to 7 weeks in a warm room

The formation of the eyes in the appropriate locations (eye nuclei) was monitored weekly during ripening in the warm room (from 2 to 7 weeks) using X-ray images. Fig. 2 shows an example (cheese 2 with PEEK tube pieces (variant PPEK 1)). The tube pieces were clearly visible on all X-ray images (Fig. 2b). The figure also shows that cheese eyes formed around the PEEK tube pieces (eye nuclei) between the third and fourth weeks in the warm room. After the fourth week, the cheese eyes in the warm room (22 °C) began to grow rapidly. These results were consistent with previous studies that described the onset of eye formation in Emmentaler cheese between days 20 and 30 (Flückiger & Walser, 1978; Pauchard, Flückiger, Bosset, & Blanc, 1980; Thierry, Salvat-Brunaud, & Maubois, 1999). The black arrows indicate three PEEK tube pieces, which are representative of all the others that were added and around which the CO_2 cheese eyes formed. No eyes formed anywhere else in the cheese. Thus, the PEEK tube pieces with their capillary cavities acted as "eye nuclei".

Two small exceptions (within the red circle) were found in Fig. 2 (week 7), very close to the border zone (cheese rind), as displayed in Fig. 2c and d. These two exceptions were not identified as genuine eye openings but as irregularities or cracks. Such cracks can occur naturally at a later stage of cheese ripening, often near the rind. Unlike the PEEK tube pieces, the PP hollow fibres were not visible by using X-ray or CT but only through micro-/macroscopy in cross-sectional views (see Section 3.3).

3.3. Monitoring eye formation at the end of the ripening period (after 100 d) using CT or cross-sectional views

Table 3 shows the analysed CT data. One main challenge of the experimental design was that the density of the PP hollow fibres and that of the PEEK tube pieces differed from the density of cheese milk. The PEEK tube pieces were easily introduced into the cheese curd, but the PP fibres were more difficult to place in the cheese curd because the majority of the hollow fibres floated on top of the whey. For this reason, the results of variants 4, 8, 12, and 16 could not be easily interpreted, especially those of variant 8 (outlier), in which many of the PP fibres were probably lost into the whey. The amount of the fibres that therefore acted as eye nuclei was difficult to control quantitatively.

The boxplots in Fig. 3 show the effects of the variants PP hollow fibres, PEEK1 (low) tube pieces and PEEK2 (high) tube pieces on eye formation in cheese and their action as eye nuclei. Two cheeses (numbers 8 and 9) were excluded from the box plots and the statistical analysis (due to the PP fibres floating on the whey and mechanical openings in a control, respectively). One control (5), one variant of PEEK1 (low) (10), and two variants of PEEK2 (high) (7, 15; the two points on the upper quartile) had higher eye volumes as a result of stronger propionic acid fermentation (see Section 3.1). They were the only cheeses with no contamination of FHL.

In this study, a two-way ANOVA showed a statistically significant effect of fibres/tube pieces (F(3, 10) = 6.8, p = 0.009) on relative eye volume (Table 3), and the effect of production day was not significant (F(1, 10) = 0.257, p = 0.62). Similar results were achieved for the effect of fibres/tube pieces (F(3, 9) = 8.0, p = 0.007) on the number of cheese eyes, and the effect of production day was not significant (F(1, 9) = 1.36, p = 0.27). Fig. 3 presents the boxplots and the corresponding pairwise comparisons after one-way ANOVA (without effect of production day).

Fig. 4a and b are the CT images and cross-sectional views, respectively. The eye formation in the controls (cheeses 1, 5, 9, and 13) was sparse. The sole exception was cheese 9 (outlier), as on the upper right side, some cheese eyes were produced by a moulding problem entrapping air in the cheese (mechanical openings). As shown in Figs. 2 and 3, although the pieces of PEEK tubes were much larger than hay particles, their capillary cavities seemed to act well as eye nuclei (cheeses 2, 3, 6, 7, 10, 11, 14, and 15) and exhibited reasonable numbers of cheese eyes. Fig. 5 presents a series of cross-sectional views at the end of ripening, with pieces of PEEK tubes or PP hollow fibres stuck into the interface of the cheese body and the cheese eyes, which formed around the tube pieces or hollow fibres during the ripening period. This indicates that they were indispensable for eye formation and acted as initialisation points of eye formation (Fig. 5a and b).

3.4. Dose response of PEEK tube pieces addition on relative eye volume and eye number

Based on SEM analysis, Guggisberg et al. (2015) postulated that the capillary microstructures from hay particles were likely to be the structural elements that act as eye nuclei in the eye formation process. The entrapment of air in capillary structures might allow the diffusion of CO_2 into intact capillaries during ripening, as proposed earlier by Martley and Crow (1996). Entrapped air greatly reduces the necessary partial pressure to start an opening. The physical principle behind trapped air in capillaries that are wetted with water or milk is capillary action, also known as capillarity (de Gennes et al., 2004; Rowlinson & Widom, 1982). Water is drawn upward in narrow tubes (capillaries) due to surface tension and adhesive forces, which can trap air bubbles. This is a result of the interaction between the surface tension, adhesion, and cohesion of the liquid with the capillary. Fig. 6 presents the linear dose response of adding PEEK tube pieces on relative eye volume and eye number, with a correlation coefficient of r = 0.79 and r = 0.77, respectively.

The findings of this study clearly indicate that PP hollow fibres and
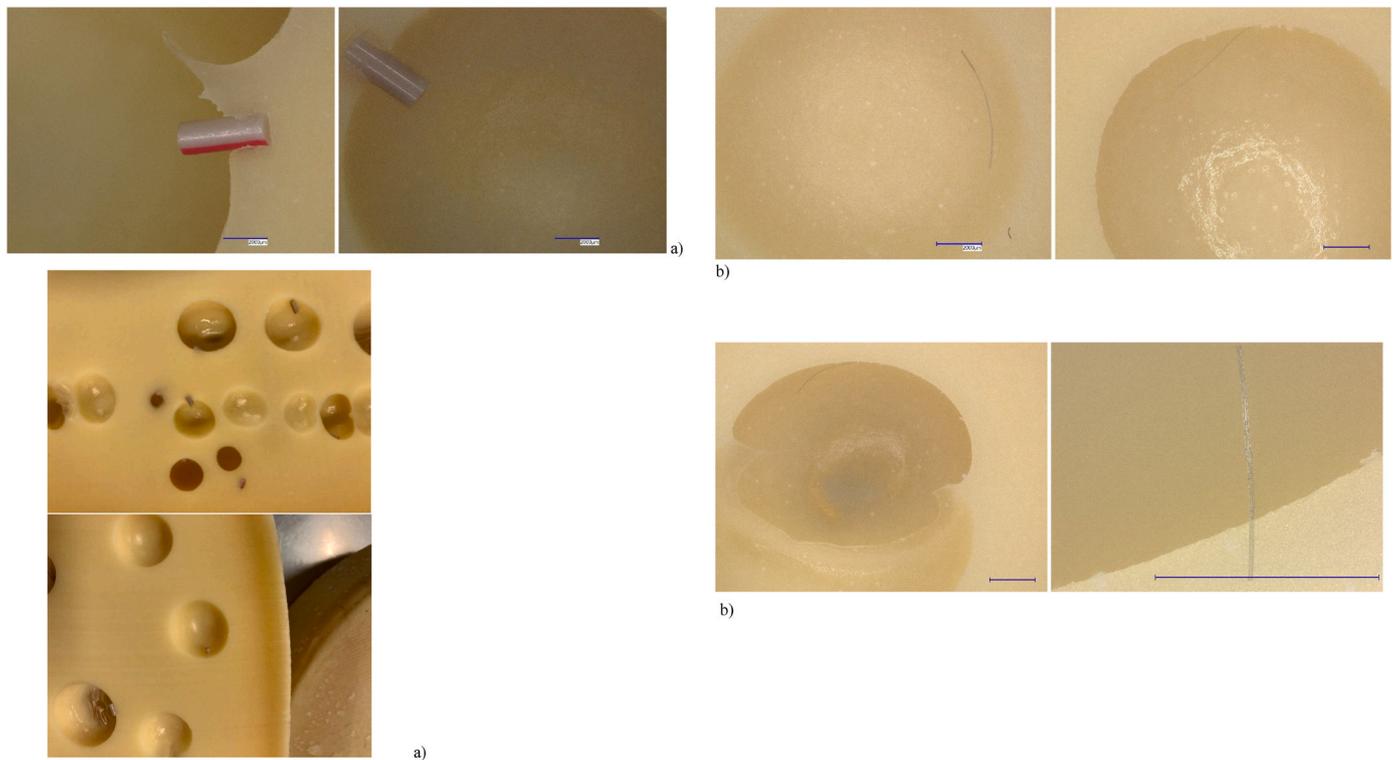
Fig. 5. Cross-sectional views of cheeses with PEEK tube pieces (a) or PP hollow fibres (b) reaching into the cheese eyes. The blue bar represents 2000 μm (2 mm). The first two and the last four pictures were taken using a Keyence microscope, whereas pictures 3 and 4 were taken using a digital camera. (For interpretation of the references to colour in this figure legend, the reader is referred to the Web version of this article.)
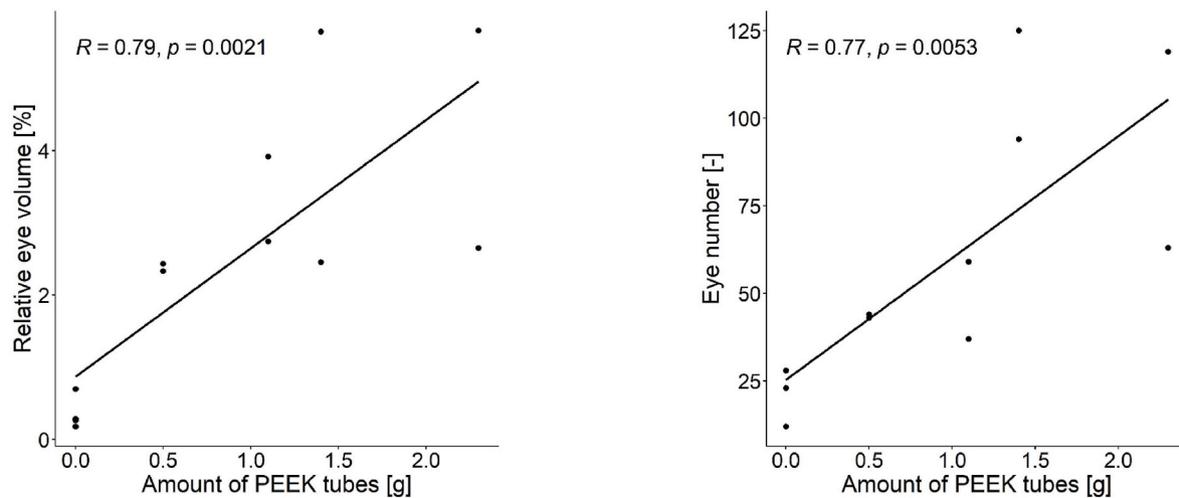
Fig. 6. Correlation between the control variants and the variants with additives of PEEK tube pieces in relation to the relative eye volume and eye numbers.

pieces of PEEK tubes containing capillaries act as eye nuclei, and this supports Guggisberg et al.'s (2015) hypothesis of microscopic, entrapped air bubbles as starting points of eye formation in cheese (Fig. 5). Guggisberg et al. (2015) described a dose-dependent response between microscopic hay particles and the relative eye volume, as well as the number of cheese eyes in experimental Emmentaler cheese. We confirmed this dose-dependent response to hay particles using PEEK tube pieces, despite the large difference in the dimensions of the hay particles and PEEK tube pieces. In a supplementary study, we tested natural products with capillary structures such as ground red clover, ground mate leaves, and ground thyme, and they all acted as eye nuclei for eye formation in cheese, with reproducible results (data not shown).

Products such as wheat fibre powder or other dry powders from ginger or potato lacking capillary cavities, however, were practically ineffective as eye nuclei, as found earlier in the study by Guggisberg et al. (2015).

4. Conclusions

Instead of natural hay particles with capillary structure elements, in the present study PP hollow fibres or pieces of PEEK tubes for experimental purposes were used to standardise the capillary cavities as eye nuclei. These applied capillaries greatly differed in their dimensions (length and inner diameter) compared to natural hay microparticles.

The dimensions proved to be irrelevant for the performance of the eye nuclei-effect. All experimentally tested synthetic capillaries enabled the eye formation process and supported the hypothesis that eye nuclei carrying entrapped air were the most likely starting points for eye formation. These findings support once more the hypothesis that natural eye nuclei are a prerequisite for eye formation in Swiss-type cheese manufacture.

CRediT authorship contribution statement

Dominik Guggisberg: Writing – review & editing, Writing – original draft, Visualization, Project administration, Methodology, Formal analysis, Data curation, Conceptualization. **Walter Bisig:** Writing – review & editing, Writing – original draft, Supervision, Project administration, Methodology, Conceptualization. **Marie-Therese Fröhlich-Wyder:** Writing – review & editing, Writing – original draft, Visualization, Supervision, Project administration, Methodology, Formal analysis, Conceptualization.

Declaration of competing interest

The authors declare that they have no known competing financial interests or personal relationships that could have appeared to influence the work reported in this paper.

Acknowledgements

Data availability

Data will be made available on request.

References

Abrahamsen, R. K., Byre, O., Steinsholt, K., & Strand, A. H. (2006). *Jarlsberg cheese history and development.* As, Norway: Tun Forlag.

Acerbi, F., Guillard, V., Aliani, M., Guillaume, C., & Gontard, N. (2016). Impact of salt concentration, ripening temperature and ripening time on CO_2 production of semi-hard cheese with propionic acid fermentation. *Journal of Food Engineering, 177*, 72–79.

Acerbi, F., Guillard, V., Guillaume, C., Saubanere, M., & Gontard, N. (2016). An appraisal of the impact of compositional and ripening parameters on CO_2 diffusivity in semi-hard cheese. *Food Chemistry, 194*, 1172–1179.

Badertscher, R., Blaser, C., & Noth, P. (2023). Validated method for the determination of free volatile carboxylic acids in cheese and bacterial cultures by GC-FID after esterification in aqueous extract and headspace injection. *Food Chemistry, 398*, 1–6.

Bisig, W., Guggisberg, D., Jakob, E., Turgay, M., Irmler, S., Wechsler, D., & Fröhlich-Wyder, M. T. (2019). The effect of NaCl and metabolic profile of propionibacteria on eye formation in experimental swiss-type cheese. *International Dairy Journal, 89*, 86–95.

Clark, W. M. (1917). On the formation of "eyes" in emmental cheese. *Journal of Dairy Science, 1*, 91–113.

Collomb, M., Spahni, M., & Steiger, G. (1990). Estimation of nitrogen according to kjeldahl in milk products and some of their nitrogen-containing fractions with an automatic system. *Mitteilungen aus dem Gebiete der Lebensmitteluntersuchung und Hygiene, 81*, 499–509.

de Gennes, P.-G., Brochard-Wyart, F., & Quéré, D. (2004). *Capillarity and wetting phenomena: Drops, bubbles, pearls, waves.* New York: Springer-Verlag. https://doi.org/10.1007/978-0-387-21656-0

Flückiger, E. (1980). CO_2- und Lochbildung im Emmentalerkäse. *Schweizerische Milchzeitung, 106*(71), 473–474.

Flückiger, E., & Walser, F. (1978). Beitrag zur Kenntnis der CO_2-Bildung im Emmentalerkäse vor Beginn der Propionsäuregärung. *Schweizerische Milchwirtschaftliche Forschung, 7*(1), 9–14.

Fröhlich-Wyder, M. T., Bachmann, H.-P., Bisig, W., Fritsch, L., Fuchsmann, P., Guggisberg, D., & Turgay, M. (2025). Chapter 34 – Cheeses with propionic acid fermentation. In P. L. H. McSweeney, P. D. Cotter, D. W. Everett, & R. Govindasamy-Lucey (Eds.), *Cheese* (5th ed., pp. 879–907). Academic Press. https://doi.org/10.1016/B978-0-443-15956-5.00025-7.

Fröhlich-Wyder, M. T., Bachmann, H.-P., & Casey, M. (2002). Interaction between propionibacteria and starter/non-starter lactic acid bacteria in swiss-type cheeses. *Le Lait, 82*, 1–15.

Fröhlich-Wyder, M. T., Guggisberg, D., Bisig, W., Jakob, E., & Schmidt, R. S. (2023). The total eye volume of cheese is influenced by different fat levels. *International Dairy Journal, 144*, 1–9.

Fragnière, C., & Schafroth, K. (2004). Neue Erkenntnisse zur Lochbildung in Käse aus mikrofiltrierter Milch. *Schweizerische Milchzeitung, 130*, 7.

Guggisberg, D., Schuetz, P., Winkler, H., Amrein, R., Jakob, E., Fröhlich-Wyder, M. T., Irmler, S., Bisig, W., Jerjen, I., Plamondon, M., Hofmann, J., Flisch, A., & Wechsler, D. (2015). Mechanism and control of the eye formation in cheese. *International Dairy Journal, 47*, 118–127.

Huc, D., Mariette, F., Challois, S., Barreau, J., Moulin, G., & Michon, C. (2014a). Multi-scale investigation of eyes in semi-hard cheese. *Innovative Food Science & Emerging Technologies, 24*, 106–112.

Huc, D., Moulin, G., Mariette, F., & Michon, C. (2013). Investigation of curd grains in swiss-type cheese using light and confocal laser scanning microscopy. *International Dairy Journal, 33*, 10–15.

Huc, D., Roland, N., Grenier, D., Challois, S., Michon, C., & Mariette, F. (2014b). Influence of salt content on eye growth in semi-hard cheeses studied using magnetic resonance imaging and CO_2 production measurements. *International Dairy Journal, 35*, 157–165.

Jakobsen, M., Jensen, P. N., & Risbo, J. (2009). Assessment of carbon dioxide solubility coefficients for semihard cheeses: The effect of temperature and fat content. *European Food Research and Technology, 229*, 287–294.

Lamichhane, P., Sharma, P., Kelly, A. L., Risbo, J., Rattray, F. P., & Sheehan, J. J. (2021). Solubility of carbon dioxide in renneted casein matrices: Effect of pH, salt, temperature, partial pressure, and moisture to protein ratio. *Food Chemistry, 336*, 1–7.

Laridon, Y., Grenier, D., Doursat, C., Huc, D., Roland, N., Flick, D., & Lucas, T. (2020). Growth of a single bubble in semi-hard cheese: Comparison between simulation and experiment. *Food Research International, 129*, 1–9.

Martley, F. G., & Crow, V. L. (1996). Open texture in cheese: The contributions of gas production by microorganisms and cheese manufacturing practices. *Journal of Dairy Research, 63*, 489–505.

Pauchard, J. P., Flückiger, E., Bosset, J. O., & Blanc, B. (1980). CO_2-Löslichkeit, -Konzentration bei Entstehung der Löcher und -Verteilung im Emmentalerkäse. *Schweizerische Milchwirtschaftliche Forschung, 9*(4), 69–73.

Rowlinson, J. S., & Widom, B. (1982). *Molecular theory of capillarity.* Mineola, New York: Dover Publications, Inc.

Schuetz, P., Guggisberg, D., Fröhlich-Wyder, M. T., & Wechsler, D. (2016). Software comparison for the analysis of cheese eyes in X-ray computed tomography. *International Dairy Journal, 63*, 62–69.

Schuetz, P., Guggisberg, D., Jerjen, I., Fröhlich-Wyder, M. T., Hofmann, J., Wechsler, D., Flisch, A., Bisig, W., Sennhauser, U., & Bachmann, H.-P. (2013). Quantitative comparison of the eye formation in cheese using radiography and computed tomography data. *International Dairy Journal, 31*, 150–155.

Thierry, A., Salvat-Brunaud, D., & Maubois, J. L. (1999). Influence of thermophilic lactic acid bacteria strains on propionibacteria growth and lactate consumption in an emmental juice-like medium. *Journal of Dairy Research, 66*, 105–113.

Wenzel, C., Irmler, S., Bisig, W., Guggisberg, D., Roetschi, A., Portmann, R., Wechsler, D., & Fröhlich-Wyder, M. T. (2018). The effect of starters with a functional arginine deiminase pathway on cheese ripening and quality. *International Dairy Journal, 85*, 191–200.